JOURNAL OF AIRCRAFT
Vol. 31, No. 4, July–Aug. 1994

Steady and Unsteady Pressure Distributions on an F/A-18 Wing at $\alpha = 30$ Deg

B. H. K. Lee,* N. R. Valerio,† and F. C. Tang‡
Institute for Aerospace Research, National Research Council, Ottawa K1A 0R6, Canada

The aim of this investigation is to provide a better understanding of the structure of the flowfield on the wing upper surface of an F/A-18 at high angles of attack. Time-averaged and rms pressure distributions were determined for different angles of attack. Spectral analyses of the pressures at different locations on the wing were carried out. Broadband space-time correlation of the pressure transducer signals was performed and the convection pattern of the pressure field was compared to the direction of the skin friction lines obtained from flow visualization studies using oil dots deposited on the wing surface.

Nomenclature

C_p = time-averaged pressure coefficient
C_p' = rms value of pressure coefficient, p_{rms}/q
$\bar{c}$ = wing mean aerodynamic chord, 8.29 in.
f = frequency, Hz
k = nondimensional frequency, fL/U_∞
L = characteristic length, in.
M = freestream Mach number
p_L = pressure on wing lower surface, psi
p_{rms} = rms value of pressure, psi
p_U = pressure on wing upper surface, psi
q = freestream dynamic pressure, psi
$R(a, b, \tau)$ = correlation of functions a and b
$R_{e\bar{c}}$ = Reynolds number based on $\bar{c}$
U_∞ = freestream velocity, ft/s
α = angle of attack, deg
τ = time delay, ms

Introduction

THE flow past an aircraft at high angles of attack has large regions of separated flows on the wings and the body. As a result, the loads at the aft fuselage and vertical fins of twin tail fighter aircraft such as the F/A-18 have been found to be unacceptably large. An understanding of the structure of the flowfield in this flight regime is important to the design of the next generation of fighter aircraft.

In the U.S., the high alpha technology research program was initiated a few years ago to provide aerodynamic data for the design of highly maneuverable aircraft. The flow visualization studies from flight tests conducted at the NASA Dryden Flight Test Center[1] provided some very illuminating information on the vortical flow generated by the forebody and leading-edge extension (LEX) of an F/A-18 aircraft. The NASA Ames Research Center has conducted wind-tunnel investigations using a full-scale F/A-18 for forebody flow control and vertical tail buffet studies.[2] Scale models of the F/A-18 have been tested in the NASA Langley wind tunnels to study the effect of vortex flow characteristics on tail buffet.[3] Numerical algorithms for predicting the flow over the F/A-18 at the high alpha flight regime have been proposed by Rizk et al.[4] and Cummings et al.[5] Computed flow patterns over the aircraft forebody, LEX, and wing surfaces, have been published for some limited flow conditions. This CFD code has not been fully validated due to the lack of available experimental data. To date, detailed experimental investigations of wing surface pressures and their statistical properties have not been conducted.

In the Canadian Forces the operational usage of the F/A-18 was considerably harsher than the original design assumptions, to the point where the life of the aircraft was substantially reduced from the original 6000 h. A structural test program was initiated in Canada to ensure the continued airworthiness of the CF-18 under current operating conditions and to provide engineering data to allow for efficient life cycle management decisions. The center fuselage was particularly critical and there was a need to carry out sufficient engineering analysis and testing. Loads data for selected critical maneuvers were needed and it was deemed that wind-tunnel tests would provide the most reliable results in the high-angle-of-attack range of the load spectra.

A rigid 6% scale model of the F/A-18 was instrumented with pressure transducers on the starboard wing and LEX, and tests were performed in the Institute for Aerospace Research (IAR) 1.5-m trisonic blowdown wind tunnel. The aim of the present study is to expand the knowledge of high-angle-of-attack aerodynamics by investigating the pressure field on the wing surface. Analysis of steady and unsteady pressures gives valuable insight on the structure of separated flows at high angles of attack. These measurements will be used for CFD code validation and also in load predictions for aft fuselage structural analysis. There are a number of ongoing programs in various NASA research centers to measure wing surface pressures on the F/A-18. The results from the present wind-tunnel studies will complement those that will be obtained shortly from NASA. Scale effects and static aeroelastic effects can be investigated from comparison of the data with those for the full-scale tests at NASA Ames.

Facility, Model, and Instrumentation

Facility

The tests were conducted in the transonic test section of the IAR 1.5-m trisonic blowdown wind tunnel. This facility has a Mach number range from $M = 0.1$–4.2. For subsonic and transonic testings, a hydraulically driven Mach number control system sets the desired test section Mach number to an accuracy of ± 0.003 over a wide angle-of-attack range of

Received July 7, 1993; presented as Paper 93-3468 at the AIAA 11th Applied Aerodynamics Conference, Monterey, CA, Aug. 9–11, 1993; revision received Sept. 28, 1993; accepted for publication Sept. 28, 1993. Copyright © 1993 by the American Institute of Aeronautics and Astronautics, Inc. All rights reserved.

*Senior Research Officer, High Speed Aerodynamics Laboratory; also Adjunct Professor, Department of Mechanical Engineering, University of Ottawa, Ottawa, Ontario K1N 6N5, Canada. Associate Fellow AIAA.

†Guest Worker, Department of Mechanical Engineering, McGill University, Montreal, Quebec H3A 2K6, Canada.

‡Associate Research Officer, High Speed Aerodynamics Laboratory.

the model pitch motion. The stagnation pressure can be maintained constant to an accuracy of ±0.02 psia throughout a wind-tunnel run. The walls of the test section are perforated with 0.5-in.-diam holes inclined at 30 deg to the flow direction, thus allowing pressure and flow communication between the test section and a 12-ft-diam, 16-ft-long plenum chamber. The wall porosity is adjustable between 0.5 and 6% of the wall area. It was set at 4% for the present measurements. At this porosity setting, the test section centerline C_p' is approximately 0.01 at $M = 0.6$.[6] The model was mounted on a cranked sting that forms part of the model support system. The strut can be programmed to move vertically and with the pitch linkage mechanism, the model angle of attack can vary from 0 to 33 deg. Under aerodynamic loading, sting bending has to be taken into consideration and this can result in an increment in the angle of attack of up to 2 deg.

The tests were carried out at different Mach numbers and angles of attack, but only results at $M = 0.6$ are presented in this article. The Reynolds number based on the model mean aerodynamic chord and the dynamic pressure corresponding to this Mach number are 3.38×10^6 and 3.95 psia, respectively.

Model

The model used in this study was a rigid 6% scale of the F/A-18. It consisted of three major pieces: 1) an aluminum forebody with integral leading-edge extension and a single place canopy; 2) a stainless steel center fuselage with integral wings; and 3) a stainless steel rear fuselage. These parts were made with close tolerance spigotted joints and were doweled and bolted together. The center fuselage was bored to accept a 1.5-in.-diam, six-component sting balance. AIM-9 missiles were mounted on the wingtips. Leading- and trailing-edge flaps were fastened to the wings by simple bolted lap joints. For the present investigation, the leading- and trailing-edge flap angles were set at 34 and 0 deg, respectively. The horizontal stabilators were set at −9 deg. These angles corresponded to the flap settings taken from the F/A-18 auto flaps-up mode schedule at high angles of attack. Boundary-layer transition trips were installed on the wings, LEX, fins, stabilators, and forebody of the model. A more detailed description of the model is given in Ref. 7.

Figure 1 shows the locations of the pressure transducers on the starboard wing and LEX. The transducers were mounted directly opposite to each other on the upper and lower surfaces. Thirty of them were installed on the LEX and 138 were spaced on eight rows along the wing span. The transducers were flush-mounted piezoresistive sensors (chips from Kulite XCQ-062-50A transducers) with an active area of 0.035 in. diam, and a frequency response above 50 kHz. In preparation for the installation of the transducers, pockets with dimensions of $0.06 \times 0.10 \times 0.015$ in. deep were machined on the wing and LEX surfaces to accommodate the chips. Trenches were also machined on the wing surfaces for the electrical wirings that were gathered in a cavity inside the fuselage and connected via cables housed in the interior of the sting support to the wind-tunnel control room. A silastomer was used to fill the holes after the chips were mounted and, at the same time, served to protect the transducers. The trenches were covered with an epoxy compound and hand-finished to give a wing profile practically the same as the original wing. Figure 2 depicts the layout of the trenches on the upper surface of the wing. In Fig. 3, a set of leading-edge flaps are shown. Matching pairs of miniature connectors were installed on the main wing and flaps to connect the flap transducers to wirings imbedded in a trench along the hinge line of the wing.

Transducer Calibration

The transducers were calibrated by mounting the F/A-18 model in a steel chamber with accurate temperature and pressure control. The calibration was carried out at a constant temperature and the pressure was varied from 5 to 30 psia in steps of 5 psia. The temperature inside the chamber was set at different values (from 5 to 45°C) in order to provide corrections to the transducer outputs during a wind-tunnel run when the temperature of the flow changes. A least-square linear fit of the transducer voltages with respect to the chamber pressure was performed. For a transducer excitation voltage of 10 V and a model temperature of 30°C, the calibration factors for the transducers were typically between 1.50–2.10 mV/psi, and the offsets between −2 and 2 psia. The average magnitude of both the calibration factor and offset sensitivity to temperature was found to be 0.03%/°C full-scale, where the transducer full-scale value is 50 psi.

The transducers were sensitive to strain effects due to deformation of the wing under aerodynamic loadings. Wind-off tests were conducted by loading the wing with a concentrated load at the tip missile launcher. The maximum load applied was 70 lb. Strain gauges were installed on the wing upper

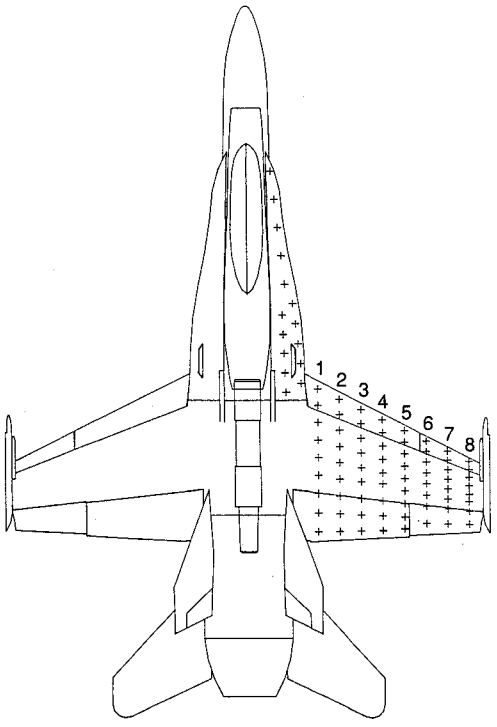

Fig. 1 Location of pressure transducers.

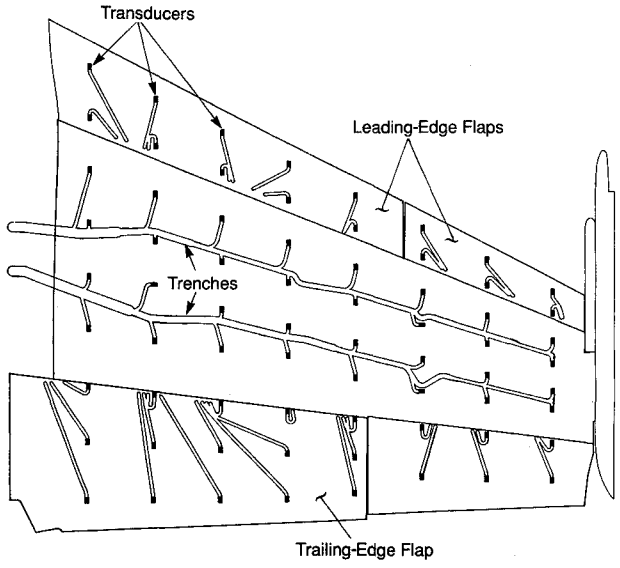

Fig. 2 Schematic of the layout of trenches for transducer wirings.

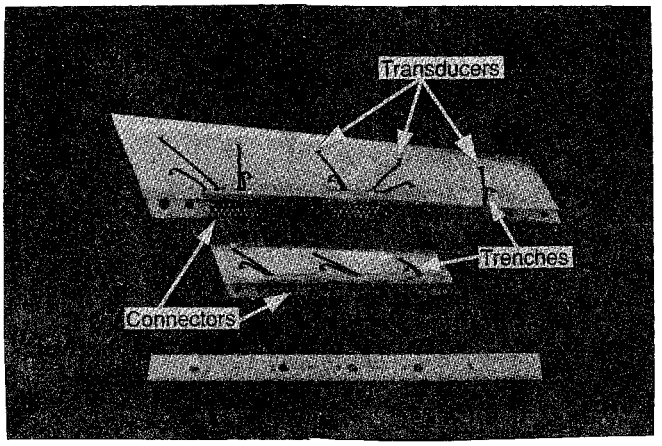

Fig. 3 Leading-edge flaps showing transducers, trenches, and connectors.

surface at five locations to measure the strain. The transducers' outputs were recorded for different values of the applied load. The strain measurements were used to validate a structural finite element model of the wing that included the cutouts for the transducers and trenches. The results from the strain analysis will be used in the future to correct for base strain effects on the transducers.

A wind-tunnel run was carried out to investigate the effect of strain on the transducers' outputs when the wing was under distributed loads. Fifteen transducers on the wing upper surface where the strain was suspected to be large were capped with brass cylinders with dimensions of 0.3 in. diam and 0.05 in. in height. The caps were glued over the selected transducers to form an airtight seal. A cavity of 0.2 in. diam and 0.031 in. deep provided a small volume of air at atmospheric pressure that was sensed by each of the 15 transducers. During the wind-tunnel run, a temperature drop of 6°C was recorded and the pressure of the trapped air in the cavities were corrected for temperature variations. The differences between the pressures measured by the transducers and the cavities' temperature corrected pressure values were attributed to strain effects. The wind-tunnel run was performed at $M = 0.6$, $q = 4.92$ psia, and α varied between 6–33 deg in steps of 5 deg. At the highest value of α where the strain was the largest, the error in readings from the transducers due to base strain effects was approximately $\pm 3\%$. The rms values obtained from these transducers were typically 0.04 psi ($C_p' = 0.008$), and the errors due to base strain have the same order of magnitude as the steady pressure measurements.

The pressure results presented in this article are not corrected for strain effects. The structural finite element model will be used in the future to determine the strain from the uncorrected pressure measurements and correction factors will then be applied to give more accurate pressure readings.

Data Acquisition System

Wind-tunnel run conditions, model angle of attack, and other parameters were recorded at 100 Hz using a PDP 11/73 computer-based wind-tunnel data system. This computer system also controlled the wind-tunnel operation and model positions. A microVax-based data acquisition system was used to collect data at a much higher sampling rate for unsteady pressure measurements. This data system consisted of a front end, a digital concentrator, and a parallel disk. The front end were blocks of instrumentation amplifiers, A/D converters, and filter/rms modules. The digital concentrator provided the link between the front end and the parallel disk. It accepted serial data from all the A/D converters and transformed them to parallel data. The data could bypass the host computer and be written directly onto the disk through an interface port on the disk drive system. The sampling frequency was set at 38.4 kHz and the data system was capable of collecting up to 10 million samples per second. The parallel disk has a capacity of 6.5 Gbytes that was sufficient to hold data acquired from an average day's wind-tunnel runs. A typical wind-tunnel run generated approximately 400–600 Mbytes of data. The data was transferred onto an 8-mm data cartridge overnight and the parallel disk was ready to accept data again the next day. Offline data processing was performed using an HP RISC 9000/750 workstation.

Results and Discussion

Surface Flow Visualization

For flow visualization studies, oil dots using SAE 30 grade motor oil mixed with carbon black were deposited on the upper surface of the uninstrumented port side wing. To achieve good visualization results, the oil dots were spaced sufficiently far apart so that the oil flow at the start of a wind-tunnel run would not interfere with the streaks when steady flow was established. This resulted in some loss of resolution in regions of rapid spatial changes in flow structure. The oil dot size used in this investigation was approximately 0.03 in. diam and spaced 0.4 in. apart in a square grid over most of the wing. At the leading edge and near the tip missile launcher, smaller dots were used and they were approximately 0.02 in. diam and spaced 0.2 in. apart. Best results were achieved for a wind-tunnel run of 30 s duration at $M = 0.6$. To obtain a permanent record of the flow visualization, white paper with an adhesive backing, such as that used for labels, was put on the wing surface after a wind-tunnel run. Care was exercised so that no air pockets were formed between the paper and the wing surface. In removing the paper, uniform tension was applied so that the paper would not be overstretched. By using label papers with different adhesive backings, a suitable one was found to give the best results for this particular model surface finish. This technique could transcribe the very fine details of the oil dot streak lines onto the paper and was found to be much better than the usual procedure of photographing the streaklines on films.

At high angles of attack, the flow on the upper surface of the F/A-18 wing was found to be very complex.[1] Regions of separation and reattachment on the inboard leading-edge flap and close to the missile launcher were observed. Figure 4

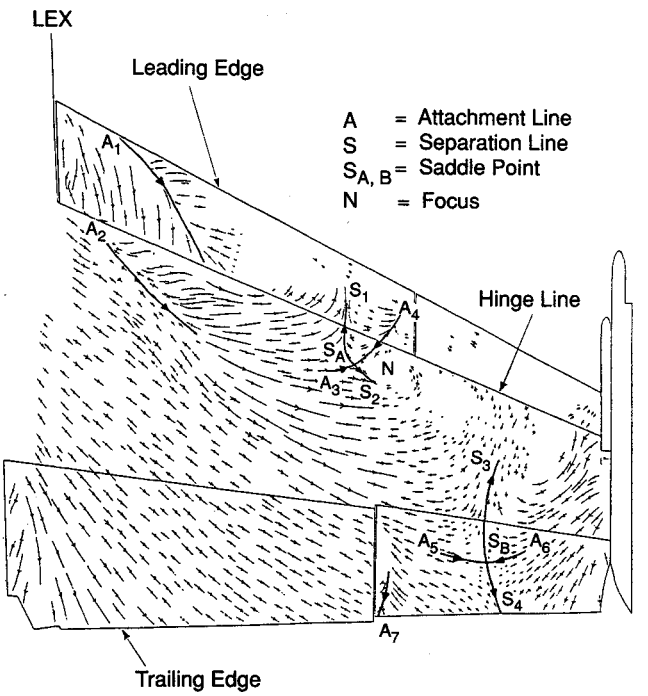

Fig. 4 Streak lines from oil dots at $M = 0.6$ and $\alpha = 30$ deg.

gives the topology of the flow on the wing surface at M = 0.6 and α = 30 deg deduced from the skin friction lines. The figure was obtained from the original oil dots record after removing the streak lines due to the starting flow. It can be seen from the streak line pattern that strong outflow dominated a major portion of the wing.

On the inboard leading-edge flap, flow separation occurs on a large portion of the flap. The flow separates close to the LEX and reattaches along the line A_1, which can be identified by a diverging pattern of the streak lines. This line approaches the hinge line and there is a region on the leading-edge flap where the surface flow cannot be determined by the oil dot streak lines. Separation also occurs along the hinge line with the flow reattaching along A_2. Only part of this line can be traced from the diverging streak lines pattern. Flow reversal on the inboard leading-edge flap is observed. A saddle point S_A, comprising the attachment lines A_3 and A_4 and separation lines S_1 and S_2 can be constructed. A focus N similar to that deduced from the tufts motion observed in flight tests[1] can be inferred from the spiraling pattern of the streak lines. The oil at the outboard leading-edge flap did not flow well and the skin friction lines were difficult to detect. A less viscous oil would probably give better results in this region.

A second saddle point S_B is found on the aileron. The streak lines near the wingtip in the vicinity of the missile launcher do not provide sufficient details to show the existence of a focus that was observed in Ref. 1. However, there are indications from this figure that a vortex is present.

At α = 25 and 35 deg, similar flow patterns were observed except that the saddle point S_A was not visible as in the α = 30-deg case. The saddle point S_B moved closer to the aileron hinge line for increasing values of α.

Analysis of Pressure Field

Figure 5 gives the steady pressure contours on the wing upper surface at M = 0.6 and α = 30 deg. The C_p distributions on the inboard leading-edge flap show a low-pressure region corresponding to the separated flow region illustrated in Fig. 4. The pressures on a large portion of the wing surface are fairly uniform rising gradually towards the trailing edge. Near the two saddle points given in the previous figure, the steady-state pressures do not show any significant changes that can be detected from the contour plots.

The rms values of the pressure fluctuations are shown in coefficient form in Fig. 6. A region of relatively large pressure fluctuations can be seen orginating from the hinge line of the leading-edge inboard flap where the flow separates. This region extends diagonally across the wing and terminates at the tip missile launcher. The largest fluctuations are observed near the trailing-edge of the aileron. For the other values of α investigated, both steady and rms pressure distributions show similar distributions.

Previous investigations of the unsteady pressures on the vertical fin and in the flowfield behind it[7,8] showed that at high angles of attack, when the LEX vortex breakdown occurs upstream of the tail, the power spectral densities (PSD) exhibit a broadband peak with center nondimensional frequency k between 0.45–0.5. Using the procedure described in Refs. 7 and 8 to compute PSD, Fig. 7 shows the results at three transducers' locations that give a fair representation of the behavior of the unsteady pressures on the main wing. The fast Fourier transform (FFT) block size used was 8192, and a Hamming window was applied to the data. Ten s of data were analyzed, and using an overlap of 50%, the number of

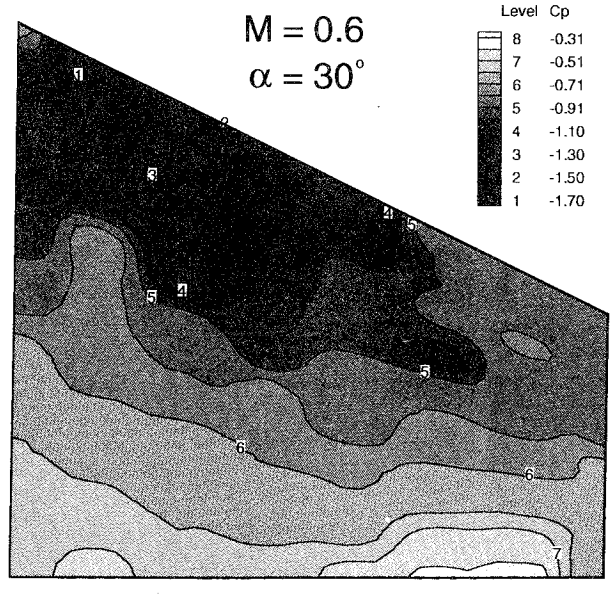

Fig. 5 Steady pressure contours on wing upper surface at M = 0.6 and α = 30 deg.

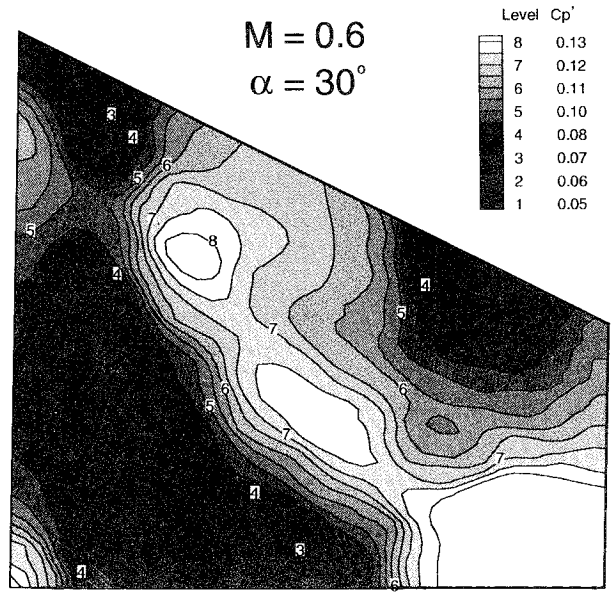

Fig. 6 Root-mean-square pressure contours on wing upper surface at M = 0.6 and α = 30 deg.

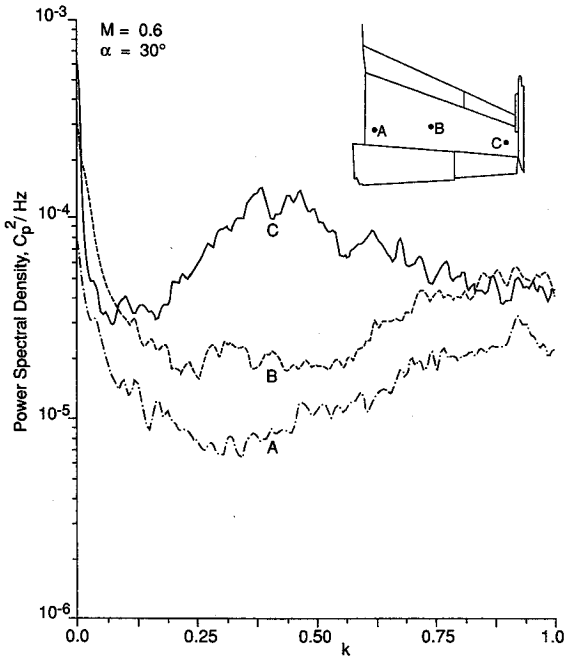

Fig. 7 Power spectral density at three transducer locations.

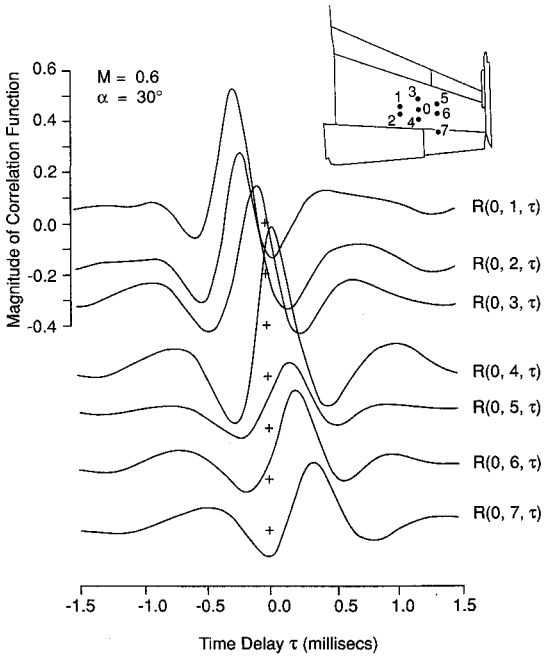

Fig. 8 Normalized cross-correlation functions.

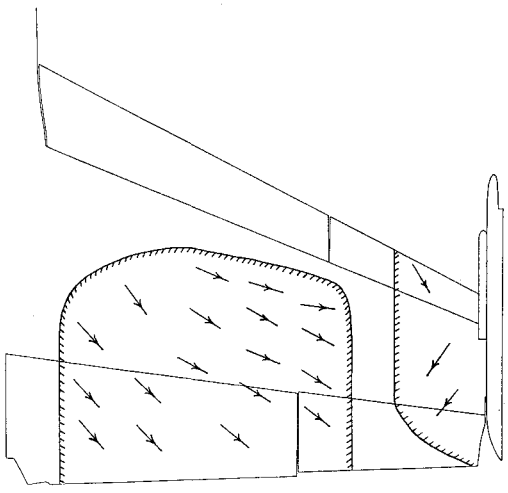

Fig. 9 Convection pattern of pressure field.

averages was approximately 190. The mean aerodynamic chord was used as L in determining k. Transducer A is the sixth transducer measured from the leading edge on the first row of transducers closest to the wing root. Transducers B and C are the fifth sensors on rows 4 and 8, respectively. The spectra do not show the broad peak that was present in the PSD plots obtained from the vertical fin pressure measurements in Ref. 7. The value of k determined from the vertical fin experiments was computed using the fin mean aerodynamic chord (5.03 in.) as L. The value of k corresponding to $L = 8.29$ in. would be between 0.74–0.82. However, a broad peak with a center frequency of approximately 0.4 is seen near the wingtip. The origin of this peak is probably due to the vortical flow generated near the tip missile launcher.

Cross-correlation studies were carried out where each transducer was taken as the reference, and time correlations were performed with respect to the transducers adjacent to it. Typical normalized correlation functions with respect to the amplitude of its autocorrelation function at $\tau = 0$ are shown in Fig. 8. The reference transducer is the fifth one in the chordwise direction on the fifth row of transducers. The transducers' pairs are marked in the inset and each curve is displaced two units downwards to avoid overlapping. Knowing the distances between the transducers and τ when the peak correlation is detected at the transducers, the broadband eddy convection velocity can be determined.

The results show that at $M = 0.6$ and $\alpha = 30$ deg, pressure correlation is found to be good in certain regions on the wing surface, and the correlation distance extends approximately 8–15% of the wing mean aerodynamic chord from the reference transducer in all directions. Using the velocities computed from each transducer pair, an approximate indication of the convection pattern can be constructed. Figure 9 shows the direction of the convection of the broadband eddies in regions on the wing surface where cross-correlation is considered good, as marked in the figure by the shaded boundaries. These two regions are separated by the sixth and seventh row of transducers. On the leading-edge flaps and in the regions where the saddle point S_A and attachment lines A_1 and A_2 are located (Fig. 4), the correlation is poor. On either side of the separation lines S_3 and S_4 orginating from the saddle point S_B, good correlation is detected, but across these two separation lines, there appears to be poor correlation. The transducers' spacings between the two regions with good correlation marked in Fig. 9 are not sufficiently close to enable detailed investigation of the flow structure. On comparing the convection pattern with the flow visualization from the oil dots experiment shown in Fig. 4, the surface streamlines and the pressure eddies move in a similar pattern.

Conclusions

The flow past the wing upper surface of a rigid 6% scale model of an F/A-18 wing was investigated from pressure measurements and oil dots flow visualization studies. The effects of Mach number and angle of attack were studied and only the results for $M = 0.6$ and $\alpha = 30$ deg are presented in this article. The flowfield at this test condition is similar to those at different M and α in the high-angle-of-attack regime.

Flow visualization from the oil streaks shows the locations of vortices and regions of flow separation and reattachment at the inboard leading-edge flap. These agree qualitatively with observations reported on the HARV in flight tests carried out at the NASA Dryden Flight Test Center. A region of fairly large pressure fluctuations originating from the leading-edge hinge line and extending to the trailing edge of the aileron is detected. This is also observed for tests carried out with α greater than 25 deg at $M = 0.6$.

At $\alpha = 30$ deg, the LEX vortex burst occurs upstream of the wing. Previous studies of the pressure field on and behind the vertical fin show the presence of a broad peak with a center frequency that is a characteristic of the LEX vortex breakdown phenomenon. Spectral analyses of the wing pressures do not show the presence of a broad peak that can be attributed to the LEX vortex burst.

Space-time correlation of the pressure transducers' outputs show two regions where good correlation is observed. The deduced convection pattern of the pressure field agrees with the direction of the streak lines obtained from flow visualization studies.

Acknowledgments

The authors wish to acknowledge the financial support from the Institute for Aerospace Research, the Department of National Defence and the Natural Sciences and Engineering Research Council of Canada. They are thankful to M. Polsenski, F. Ellis, and J. Bureau for their assistance.

References

[1]Fisher, D. F., Del Frate, J. H., and Richwine, D. M., "In-Flight Flow Visualization Characteristics of the NASA F-18 High Alpha Research Vehicle at High Angles of Attack," NASA TM 4193, May 1990.

[2]Meyn, L. A., Lanser, W. R., and James, K. D., "Full-Scale High

Angle-of-Attack Tests of an F/A-18," AIAA Paper 92-2676, June 1992.

[3]Shah, G. H., "Wind-Tunnel Investigation of Aerodynamic and Tail Buffet Characteristics of Leading-Edge Extension Modifications on the F/A-18," AIAA Paper 91-2889, Aug. 1991.

[4]Rizk, Y. M., Schiff, L. B., and Gee, K., "Numerical Simulation of Viscous Flow Around a Simplified F/A-18 at High Angle of Attack," AIAA Paper 90-2999, Aug. 1990.

[5]Cummings, R. M., Rizk, Y. M., Schiff, L. B., and Chaderjian, N. M., "Navier-Stokes Predictions for the F-18 Wing and Fuselage at Large Incidence," *Journal of Aircraft*, Vol. 29, No. 4, 1992, pp. 565–574.

[6]Ohman, L. H., and Brown, D., "Performance of the New Roll-in Roll-out Transonic Test Section of the NAE 1.5M × 1.5M Blow-down Wind Tunnel," *Proceedings of the 17th Congress of the International Council of the Aeronautical Sciences* (Stockholm, Sweden), 1990, pp. 363–387.

[7]Lee, B. H. K., and Brown, D., "Wind-Tunnel Studies of F/A-18 Tail Buffet," *Journal of Aircraft*, Vol. 29, No. 1, 1992, pp. 146–152.

[8]Lee, B. H. K., Brown, D., Tang, F. C., and Plosenski, M., "Flow-field in the Vicinity of an F/A-18 Vertical Fin at High Angles of Attack," *Journal of Aircraft*, Vol. 30, No. 1, 1993, pp. 69–74.

AEROSPACE FACTS AND FIGURES, 1993-1994

This book, published by Aerospace Industries Association, is the most complete one-stop data source on the U.S. aerospace industry that you'll find. It features more than 140 statistical tables showing trends over time in the U.S. aerospace industry. Tables are updated through 1992. Selected tables include 1993 and 1994 estimates based on U.S. government budget projections.

You'll find updates on aerospace sales; shipments, orders, and backlog of aircraft, engines, and parts; production of U.S. civil and military aircraft; outlays for missile procurement by military service; space activities outlays by federal agency; world and U.S. aircraft fleet data; aerospace R&D funding; U.S. aerospace trade; U.S. aerospace employment by sector; aerospace profits, capital investment, and industry balance sheets.

1993, 176 pp, Paperback
$25.00 each
Order #: AFF-94(945)

Place your order today! Call 1-800/682-AIAA

AIAA
American Institute of Aeronautics and Astronautics

Publications Customer Service, 9 Jay Gould Ct., P.O. Box 753, Waldorf, MD 20604
FAX 301/843-0159 Phone 1-800/682-2422 8 a.m. - 5 p.m. Eastern

Sales Tax: CA residents, 8.25%; DC, 6%. For shipping and handling add $4.75 for 1-4 books (call for rates for higher quantities). Orders under $100.00 must be prepaid. Foreign orders must be prepaid and include a $20.00 postal surcharge. Please allow 4 weeks for delivery. Prices are subject to change without notice. Returns will be accepted within 30 days. Non-U.S. residents are responsible for payment of any taxes required by their government.